# Mechanism of Quinol Oxidation by Ferricenium Produced by Light Excitation in Reaction Centers of Photosynthetic Bacteria

**ARTICLE** *in* THE JOURNAL OF PHYSICAL CHEMISTRY B · APRIL 2007

Impact Factor: 3.3 · DOI: 10.1021/jp067834+ · Source: PubMed



**6 AUTHORS**, INCLUDING:

Francesco Milano
Italian National Research Council
**71** PUBLICATIONS **390** CITATIONS
SEE PROFILE

Angela Agostiano
Università degli Studi di Bari Aldo Moro
**358** PUBLICATIONS **4,074** CITATIONS
SEE PROFILE

László Nagy
University of Szeged
**54** PUBLICATIONS **440** CITATIONS
SEE PROFILE

Massimo Trotta
Italian National Research Council
**117** PUBLICATIONS **550** CITATIONS
SEE PROFILE

# Mechanism of Quinol Oxidation by Ferricenium Produced by Light Excitation in Reaction Centers of Photosynthetic Bacteria

**Francesco Milano,[†] László Gerencsér,[‡] Angela Agostiano,[†] László Nagy,[‡] Massimo Trotta,[†] and Péter Maróti*,[‡]**

*Instituto per i Processi Chimico−Fisici, Sede di Bari, Via Orabona 4, I-70126, Bari, CNR Via Orabona, Italy, and Department of Biophysics, University of Szeged, Egyetem utca 2, H-6722, Szeged, Hungary*

*Received: November 25, 2006; In Final Form: January 31, 2007*

The kinetics and thermodynamics of cyclic electron transfer through the isolated reaction center protein of photosynthetic bacterium *Rhodobacter sphaeroides* were determined in detergent (Triton X-100) solution. The redox reactions between the reducing (ubiquinol-0 or ubiquinol-10) and oxidizing species (ferricenium, ferricytochrome, or ferricyanide) produced chemically or by light excitation of the protein were monitored by absorption changes of the reactants and by acidification of the solution accompanied with the disappearance of the quinol. The bimolecular rate constants of reactions of anionic ubiquinol-0 with different oxidizing agents showed large variation: $5 \times 10^8$ $M^{-1}$ $s^{-1}$ for ferricenium, $3.5 \times 10^5$ $M^{-1}$ $s^{-1}$ for ferricyanide, and $1.5 \times 10^5$ $M^{-1}$ $s^{-1}$ for ferricytochrome. Although the redox partners were created in pairs by the same protein promptly after light excitation, their bimolecular redox reaction was not observed even in the case of the fastest reacting partners of ferricenium and ubiquinol-0. Instead, they equilibrate with the corresponding (donor and acceptor) pools before the electron is transferred. The (logarithms of the) observed rate constants of quinol oxidation showed steep pH-dependence for water soluble ubiquinol-0 (slope +1) and mild pH-dependence for hydrophobic ubiquinol-10 (slope ≈ 0.25). Combined with studies of the ionic strength dependence of the rate, it was concluded that the electron-transfer pathways of ubiquinol-0 and ubiquinol-10 oxidation started from their anionic and neutral forms, respectively. The mild pH-dependence of the rate of ubiquinol-10 oxidation came from the electrostatic interactions between ferricenium and the pH-dependent surface charges of the reaction center. The results help to understand, monitor, and design (cyclic) electron flow in bioenergetic proteins.

## 1. Introduction

During photosynthetic free energy conversion, the absorbed light energy generates proton motive force via coupled transmembrane electron transfer and proton translocation.[1−3] The open-chain electron transfer of oxygenic photosynthesis leads to the oxidation of water and the reduction of $NADP^+$. The light-induced cyclic electron transfer of anoxygenic photosynthesis in purple bacteria is mediated by four components: two transmembrane proteins (bacterial reaction center (RC) and cytochrome $bc_1$ complex), the ubiquinone/ubiquinol ($UQ/UQH_2$) pool, and the water-soluble protein cytochrome $c_2$ (cyt $c_2$). The light absorbed by the RC initiates multistep internal electron transfer leading to the oxidation of the bacteriochlorophyll dimer ($P \rightarrow P^+$) at the periplasmic side and reduction of the bound ubiquinone ($UQ \rightarrow UQH_2$) at the cytoplasmic side of the membrane. The ubiquinol ($UQH_2$) leaves the protein and is replaced by UQ from the quinone pool.[4] The initial redox state of the RC is established by the cyt $bc_1$ complex thereby closing the electron-transfer cycle after the following steps: $P^+$ is reduced by cyt $c^{2+}$, the cyt $c^{3+}$ is reduced by the cyt $bc_1$ complex, and concomitantly the ubiquinol is oxidized by the cyt $bc_1$ complex with simultaneous release of the protons into the periplasmic space of the bacterium.

In model systems, the cytochrome $bc_1$ complex can be absent and its function can be mimicked by large pools of quinone and electron donor in appropriate redox states. Although the electron transfer is not anymore cyclic, the properties of intraprotein electron transfer, the generation of a proton electrochemical gradient, and the turnover of the RC can be well studied.[5−9] However, under defined conditions, the electron transfer can be made cyclic if the quinol reduces directly the oxidized donor (Figure 1).[10,11]

In *in vitro* systems, even cyt $c_2$, the native electron donor to the oxidized dimer can be replaced by other redox agents. One of the most attractive organometallic compounds is ferrocene (cyclopentadienyl iron, $Fe(C_5H_5)_2$ of sandwich type structure), whose redox transition (ferricenium/ferrocene, $fcn^+$/fcn) is not accompanied with protonation changes and has negligible absorption changes in the visible spectral range. These advantages were utilized when ferrocene was used as a donor to $P^+$ to determine the stoichiometry of light-induced proton binding.[12] As the ferrocene has very low inner-sphere reorganization energy in electron transfer (0.3 kcal/mol),[13] it has been conjugated to many different biomolecules, including nucleic acids and proteins.[14]

Cyclic electron transfer around isolated RC can be generated using ferrocene as electron donor to $P^+$ (Figure 1). The key point to control the cyclic flow of electrons is the interaction of ferricenium produced by light excited RC and ubiquinol. The reaction mechanism of oxidation of ubiquinol by ferricenium

* Corresponding author. Phone: 36-62-544-120. Fax: 36-62-544-121. E-mail: pmaroti@sol.cc.u-szeged.hu.
[†] Instituto per i Processi Chimico−Fisici.
[‡] Department of Biophysics.

10.1021/jp067834+ CCC: $37.00 
Published on Web 03/30/2007

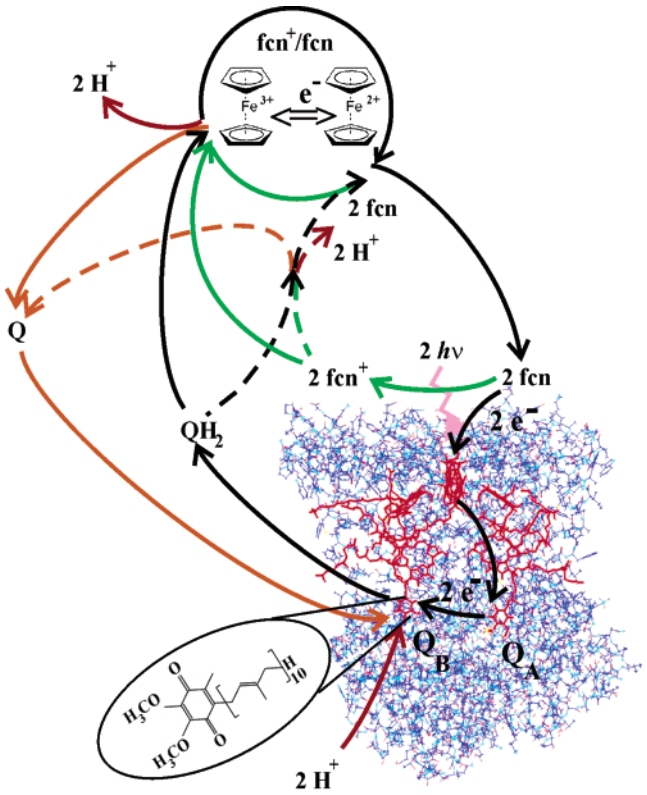


**Figure 1.** Light-induced cyclic electron-transfer mediated by pools of ferricenium/ferrocene ($fcn^+$/fcn) and quinone/quinol ($Q/QH_2$) in isolated RC from photosynthetic bacterium *Rb. sphaeroides*. Upon flash excitation ($h\nu$) of the dimer at the periplasmic side, internal electron transfer ($e^-$) is initiated that leads to reduction of the quinone at the cytoplasmic side ($Q \rightarrow QH_2$). The reset of the RC is assured by reduction of the oxidized dimer by ferrocene ($fcn \rightarrow fcn^+$) and by exchange of $QH_2$ by Q from the pools. The dissociated $QH_2$ can be oxidized by $fcn^+$ either from the pool (solid lines) or from the same protein that emerged $QH_2$ (dashed lines). The steps of quinone and ferrocene cycles are orange and green, respectively, except if they are part of the cyclic electron flow (black). Proton uptake in the RC and proton release related to quinol oxidation in the bulk are brown. The cofactors are highlighted by red. The atoms of the backbone of the RC are color coded. The chemical structures of the ubiquinone-10 in the $Q_B$ binding pocket and ferricenium/ferrocene in the pool are exposed. The details of the coupling of the one-electron oxidation of ferrocene and the two-electron reduction of quinone are omitted here (see text).

has not been investigated and needs to be solved. This will be set to the focus of our studies together with the observed instability of ferricenium in neutral and basic aqueous solutions.[14] Several observations and questions have been accumulated, which make the determination of the thermodynamic and kinetic parameters of the ferricenium/ferrocene related redox and catalytic reactions interesting and important.

(a) The reductants in the reduction of ferric cyt c by the benzoquinone/benzoquinol system were the anionic quinol ($QH^-$) and the deprotonated semiquinone anion ($Q^-$), which is formed by dismutation of the quinol and the quinone.[15] In another analogous system of menadione/menadiol, the reduction of ferric cyt c was controlled by the oxidation of the anionic quinol.[16] Some questions arise: what are the intermediate steps and what are their contributions in oxidation of ubiquinol (either native $UQ_{10}H_2$ or its water soluble analogue $UQ_0H_2$) by ferricenium generated by light excitation of photosynthetic RC?

(b) The protein generates and exports oxidizing and reducing species at the donor and acceptor sides, respectively (Figure 1). Do they interact immediately after production or does the reaction takes place only after redox equilibration with the bulk?

(c) Light-induced proton uptake measurements using either flash light[12,17] or continuous illumination,[18,19] indicating that ferrocyanide increased significantly the lifetime of the light-induced quinol in the presence of donors (e.g., ferrocene). This observation can point either to specific interaction between ferrocyanide and ferricenium formed via light excitation of the RC or to ferricyanide/ferrocyanide mediated redox control of the electron transfer from quinol to ferricenium.

(d) Finally, our studies may contribute to the realization of several nanoscale projects as conversion and storage of energy. Very recently, the mediating role of ferricenium/ferrocene was indicated in electron transfer between bacterial RC and single-walled carbon nanotubes.[20] In several photosynthetic bacteria (e.g., *Rhodopseudomonas viridis*), organometallic compounds as (cytochrome) subunits serve as well tuned electron donors to the photo-oxidized bacteriochlorophyll dimer. The artificial incorporation of ferrocene into bacterial RC without bound cytochrome seems to be a promising and interesting project. This novel protein would combine the benefits of both ferrocene (tunable redox properties) and protein (high regio- and enantioselectivity). The ferrocene−RC organometalloprotein could be an appropriate model system to study electron transfer *in vitro* and could find potential application in construction of a new biosensor of biological electron flow.

## 2. Materials and Methods

**2.1. Chemicals.** 2,3-Dimethoxy-5-methyl-1,4-*p*-benzoquinone ($UQ_0$ with no isoprene tail) (Sigma) was solubilized in water in stock solutions of 40 mM. $UQ_0$ (yellow) was reduced to $UQ_0H_2$ (colorless) under a $H_2$ gas stream in the presence of palladium black powder (surface area 40−60 $m^2/g$) as catalyst (Aldrich). It is readily soluble in water and has a large UV absorption band at 269 nm that converts to a much smaller band at 286 nm in its fully reduced form, $UQ_0H_2$ (Figure 2, top). Notice that the $UQ_0$−$UQ_0H_2$ difference spectrum has an isosbestic point at 288 nm. Due to its long isoprenoid chain, the natural quinone of the RC, ubiquinone-10, $UQ_{10}$ (Sigma), is not soluble in water. It is solubilized in a detergent system where the quinone is confined into the hydrophobic core of the micelle. $UQ_{10}$ (yellow) in ethanol was reduced to $UQ_{10}H_2$ (colorless) under a $H_2$ gas stream in the presence of palladium black. The absorption spectra of redox forms of $UQ_{10}$ in detergent of 0.03% Triton X-100 (Sigma) resemble those in 80% ethanol[21] or $UQ_0$ in water (Figure 2, top). Ferrocene (Sigma) was dissolved in ethanol (stock solution 10 mM) and used after preparation without further reduction, as its redox midpoint potential is relatively high: $E_m$ (ferricenium/ferrocene) ≈ 400 mV in water.[22,23] Ferricenium was generated by addition of 2 drops of concentrated (96%) $H_2SO_4$ into 1 mL of 10 mM ferrocene in ethanol under $O_2$ bubbling (15 min) in the presence of palladium black. The oxidation was indicated by a strong color change from yellow (ferrocene) to blue/green (ferricenium). The ferricenium/ferrocene difference absorption spectrum in water has a small band in the visible range (620 nm) and a broad band in the UV (240−310 nm) with characteristic peaks at 249 nm (larger) and 285 nm (smaller) (Figure 2, bottom). The wavelengths of 249 and 620 nm are highly suited for detection of ferricenium because the quinone and quinol have close to minimum absorption and have no absorption at all, respectively (Figure 2, top). Due to the low stability of ferricenium in water, ferricenium hexafluorophosphate ($fcn^+PF6^-$, Sigma) was used to determine the absorption coefficient at 620 nm (vs 750 nm): $\epsilon_{620}(fcn^+PF6^-) = 305\ M^{-1}\ cm^{-1}$ (10 mM

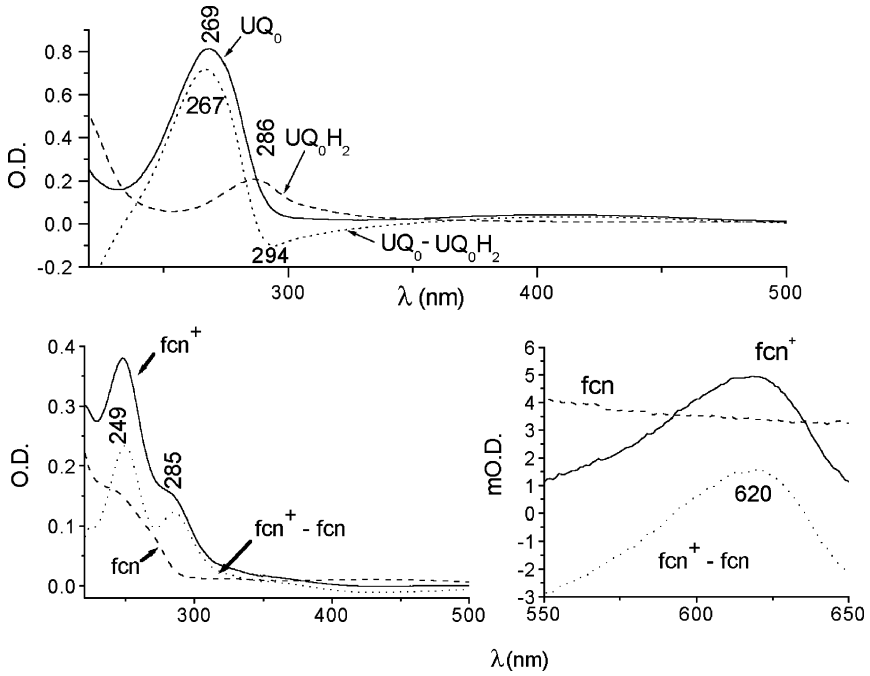


**Figure 2.** Steady-state optical absorption spectra of $UQ_0$, $UQ_0H_2$, and $UQ_0-UQ_0H_2$ (top) and ferrocene, ferricenium, and their difference on two spectral regions (bottom) in aqueous solution. Note that the $UQ_0-UQ_0H_2$ difference spectrum has a large positive peak at 267 nm, a much smaller negative peak at 294 nm, and an isosbestic point at 288 nm. The $fcn^+-fcn$ difference spectrum has two characteristic peaks in the UV region (at 249 and 285 nm) and one (much smaller) peak in the red spectral range (at 620 nm).

acetate, pH 4.75). $Fcn^+PF6^-$ can be dissolved in water up to 5 mM, and the stock is stable for 5−6 h under nonacidic conditions. Mammalian (horse heart) cytochrome c (Sigma, type VI) was reduced (>95%) by bubbling $H_2$ gas through its solution in the presence of palladium black. The concentration of reduced cyt c was obtained using an extinction coefficient of $\epsilon_{550}$-(reduced) = 27.6 $mM^{-1}$ $cm^{-1}$.[24] The pH indicator absorption dyes, phenol red, bromo-cresol purple (BCP), and *o*-cresol red (Sigma) were dissolved in ethanol and used in concentrations of 20−30 $\mu$M. The pH buffers (acetate, Mes, Mops, Phosphate, and Tris) were obtained from Sigma. All materials were used without any further purification.

**2.2. Reaction Center.** RCs were isolated from blue-green (carotenoidless) mutants (strain R-26) of photosynthetic bacterium *Rhodobacter* (*Rb.*) *sphaeroides* following established procedures using lauryldimethylamine-*N*-oxide (LDAO) extraction and were purified by ammonium sulfate and diethylaminoethyl (DEAE) chromatography.[12] The zwitterionic detergent LDAO was changed for non-ionic detergent (Triton X-100) by overnight dialysis against 1 mM Tris buffer (pH 8) at 4 °C. The OD(280 nm)/OD(802 nm) ratio, a measure of the purity of the RC, was smaller than 1.40. The concentration of the RC was determined from the steady-state absorption at 802 nm ($\epsilon$ = 288 $mM^{-1}$ $cm^{-1}$). The native ubiquinone ($UQ_{10}$) in the $Q_B$ site was extracted with 1% LDAO and 2 mM orthophenanthroline[25] and replaced by $UQ_0$ by addition of the solid quinone to the RC stock[26] or of the concentrated stock of $UQ_0$ in water. The reconstitution of $Q_B$ with $UQ_0$ was tested by detection ($\lambda$ = 450 nm) of the period of two oscillations of $Q_B^-$ upon series of saturating flashes (data not shown).

**2.3. Optical Measurements.** The kinetic traces of absorption changes were recorded using a UV−visible-NIR spectrophotometer (Cary 5000 Varian Inc.). The sample in the rectangular quartz cuvette was stirred on the bottom. The absorption transients were detected after injection and rapid (≈1 s) mixing of the reagents or after illumination from the top by saturating a Xe flash tube (FX-200 EG/G) screened with a red filter.

**2.4. Measurement of Proton Release.** The pH indicator dyes, phenol red (useful pH range 6.5−7.5 and monitoring wavelength $\lambda$ = 560 nm), *o*-cresol red (7.5 < pH < 8.5, and $\lambda$ = 572 nm), and bromo-cresol purple (BCP, 5.5 < pH < 7.5, and $\lambda$ = 579 nm) were used to follow the pH change of the solution due to proton release as a consequence of quinol oxidation. The buffering capacity of the RC solution was decreased by overnight dialysis against the solution of 0.03% Triton-X 100 and 50 mM NaCl. Ferrocene was used as external electron donor to oxidized dimer ($P^+$) because its redox change is not accompanied with protonation and has negligible absorption change upon oxidation at the wavelengths of the maximal sensitivity of the pH indicator dyes. The net proton release was obtained by subtraction of the signal of the buffered sample (10 mM buffer) from the response of the (unbuffered) dye.[12]

**2.5. Redox Titration.** The sample was kept in an airtight redox cuvette under an oxygen-free $N_2$ stream. The redox potential was measured with a platinum electrode versus the Ag/AgCl reference electrode of a combined pH electrode. The potential of the solution was varied by addition of oxidizing (air, hydrogen peroxide, and ferricyanide, $E_h$ up) and reducing (ferrocyanide and sodium dithionite, $E_h$ down) agents in the presence of stable redox mediators ($fcn^+PF6^-$/ $fcnPF6^-$ and/or ferricyanide/ferrocyanide).

**2.6. Fitting Procedures.** The initial phase of the absorption transients was approximated by a monoexponential function according to the nonlinear least-square fitting procedure by the Levenberg−Marquardt algorithm.

All measurements were performed at room temperature (23 °C).

## 3. Results

**3.1. Ferricenium/Ferrocene Redox Couple in Aqueous Solutions.** Ferrocene, one of the most widely used redox agents in chemistry,[23,27] is readily oxidized to the green/blue ferricenium cation electrochemically[14,28] or by oxidizing agents

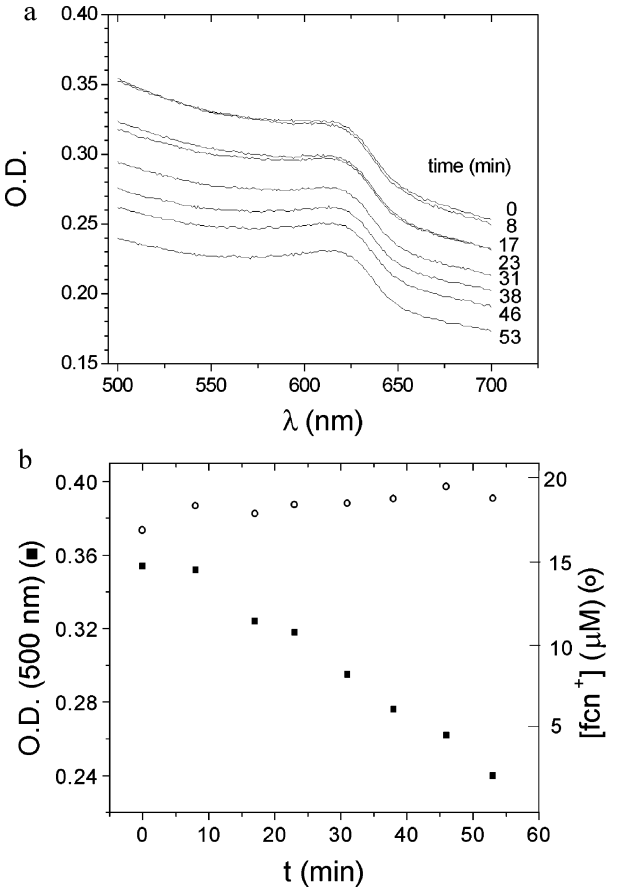


**Figure 3.** Determination of solubility of ferrocene and degradation time constant of ferricenium in aqueous solution from time-dependence of the absorption spectra of ferricenium solution (panel a) of the light scattering (500 nm, left axis of panel b) and of the ferricenium concentration (620 nm, right axis of panel b). The initial concentration of ferrocene was much above its solubility limit in water.[23,29] The measured spectra were corrected for light scattering, and the concentration of ferricenium was calculated using the extinction coefficient of 305 $M^{-1}$ $cm^{-1}$ at 620 nm. The light scattering (detected at 500 nm) reflecting the amount of undissolved ferrocene decreased as a consequence of degradation of ferricenium with a time constant of 5 h (see text for details). Conditions were as follows: 200 $\mu$M ferrocene, 2 mM ferrocyanide, 250 $\mu$M ferricyanide, $E_h$ = 381 mV (vs SHE), pH 6.7, 0.03% Triton X-100, 30 mM NaCl, and the light path 5 cm.

(typically $HNO_3$, $Ag^+$, or $I_2$). Ferricenium is a mild one-electron oxidant, but the application of the ferricenium/ferrocene redox couple in aqueous solution is highly limited. (1) The ferrocene has low solubility in water. The reported values cover a wide range from 34 to 68 $\mu$M (the results of several authors are summarized in ref 29), including 52 $\mu$M measured in various aqueous 0.1 M NaCl detergent solutions.[23] (2) The ferricenium is not stable in neutral or basic aqueous solutions. A small amount of concentrated (10 mM) ferricenium was injected and diluted to 25 $\mu$M in buffered solution (50 mM). The mixing was completed within 1 s. At pH 7.5 (Tris), the exponential decay of the characteristic 249 nm peak of the ferricenium showed a rate of 8 $s^{-1}$. At pH 6.0 (Mes), the rate of decay was smaller than the stability limit of the experimental setup (1 $min^{-1}$).

By detection of the time-dependence of the absorption spectra of the ferricenium dissolved in water, both the rate of its disappearance and the solubility limit of the ferrocene could be studied (Figure 3). Initially, the ferrocene was added in large excess (much above the solubility limit) to the aqueous solution (200 $\mu$M) at $E_h$ = 381 mV poised with ferricyanide/ferrocyanide.

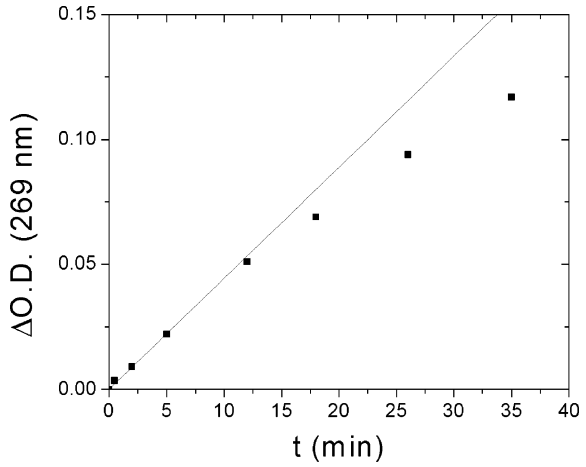


**Figure 4.** Kinetics of $UQ_0H_2$ oxidation by $UQ_0$ (dismutation) in aqueous solution detected at the absorption peak of $UQ_0$ (269 nm) after sudden mixing of reactants of equal concentrations in an UV tandem cuvette with 2 × 0.4375 cm path length. The slope of the absorption increase ($k_{obs}$ = 0.0044 OD/min) corresponds to 0.39 $\mu$M $UQ_0$/min production rate (the absorption coefficient of $UQ_0$ at 269 nm is 1.3 × $10^4$ $M^{-1}$ $cm^{-1}$) or $k'_d = 1 \times 10^{10}$ $M^{-1}$ $s^{-1}$ bimolecular rate constant (see the text). Conditions were as follows: 50 $\mu$M $UQ_0H_2$, 50 $\mu$M $UQ_0$, 50 mM phosphate buffer, pH 6.9, and 100 mM KCl.

The concentration of the ferricenium was calculated from the absorbance at 620 nm (after correction for light scattering) using the extinction coefficient of 305 $M^{-1}$ $cm^{-1}$ (see Materials and Methods). The rate of the ferrocene solubilization was inferred by the decrease of the scattering measured at 500 nm, where both the solubilized ferrocene and ferricenium have minor contributions (Figure 2). The ferrocene solubilizes to maintain the ratio of its redox forms imposed by the $E_h$ replenishing the aliquots that have been oxidized and subsequently degraded. Consequently, the decay of the light scattering represents also an estimate of the time constant of the ferricenium degradation (5 h). Under stationary conditions (pH 6.7), the concentration of the ferricenium (19 ± 1 $\mu$M) did not depend on time and $fcn^+$ could be considered as stable species. The actual ferrocene concentration (40 ± 2 $\mu$M) was calculated from the Nernst equation ($E_m(fcn^+/fcn)$ = 400 mV)[22,23] in good agreement with the solubility values reported earlier.[23,29]

**3.2. (Autocatalytic) Oxidation of $UQ_0H_2$ by $UQ_0$ in Solution.** Although the target of the present study is the oxidation of quinol by ferricenium, the possible contribution of autocatalytic oxidation of $UQ_0H_2$ was also investigated (Figure 4). The conversion of quinol to quinone was tracked at 269 nm, the peak absorption of the $UQ_0-UQ_0H_2$ difference spectrum. The solutions of $UQ_0$ (50 $\mu$M) and $UQ_0H_2$ (50 $\mu$M) containing 50 mM phosphate buffer (pH 6.9) and 100 mM KCl were placed in a UV tandem cuvette of 2 × 0.4375 cm path length (Hellma) and mixed suddenly. The observed slow and small change of the absorption ($k_{obs}$ = 0.0044 OD/min) was attributed to the autocatalytic oxidation of $UQ_0H_2$ by $UQ_0$. The slope of the absorption increase corresponded to a 0.39 $\mu$M $UQ_0$/min initial production rate (the absorption coefficient of $UQ_0$ at 269 nm is 1.6 × $10^4$ $M^{-1}$ $cm^{-1}$; see Figure 2, top). On the basis of the model of reaction pathways of quinol oxidation, the observed initial rate of quinone accumulation can be used to derive the bimolecular rate constant of the $UQ_0H_2 \rightarrow UQ_0$ redox reaction (dismutation).

**3.3. Electron Transfer from Quinol to Ferricenium in Solution.** As the protonation states of the different reduction forms of the quinone can be adjusted by the pH of the solution, the observation of the pH dependence of the rate of quinol

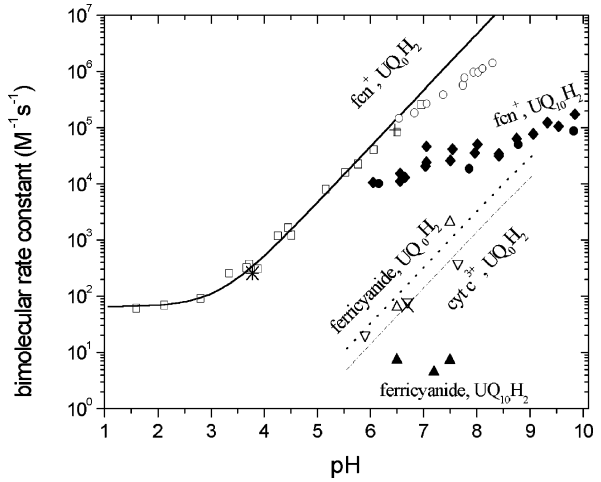


**Figure 5.** pH dependence of the bimolecular rate constant of reduction of ferricenium (□, ●, ○, ◇, and ◆), ferricytochrome (▽), and ferricyanide (▲, △) by quinol ($UQ_0H_2$ (open symbols) or $UQ_{10}H_2$ (closed symbols)) produced chemically (1) or photochemically by RC (2). (1) The reaction was initiated by rapid (<1 s) mixing of the oxidants [cyt $c^{3+}$ (13.3 $\mu$M, detected at 550 nm), ferricenium (1−40 $\mu$M, detected at 620, 285, or 249 nm) or ferricyanide (0−200 mM)] and the reductants [$UQ_0H_2$ (1−400 $\mu$M) or $UQ_{10}H_2$ (1−10 $\mu$M)]. At some pH values, the oxidation of $UQ_0H_2$ was tracked in the presence of oxidized quinone [5 $\mu$M (+), 20 $\mu$M (×), and 40 $\mu$M (*) $UQ_0$]. (2) The quinol was produced by RC after two light flashes, and its reoxidation was tracked by disappearance of ferricenium (249 nm, ◆ and ◇) or by detection of the proton release with pH indicator dyes (○, ●, and ▲). Using eq 16 with $pK_A = 10.03$ and $pK_B = 12.43$ for $UQ_0$,[32] the best fit lines to the data were drawn with bimolecular rate constants of $k'_1 = 65$ $M^{-1}$ $s^{-1}$ and $k'_2 = 5 \times 10^8$ $M^{-1}$ $s^{-1}$ for fcn$^+$ (solid line), $k'_2 = 1.5 \times 10^5$ $M^{-1}$ $s^{-1}$ for cyt $c^{3+}$ (dash-dot line), and $k'_2 = 3.5 \times 10^5$ $M^{-1}$ $s^{-1}$ for ferricyanide (dot line). The rate of oxidation of $UQ_{10}H_2$ by fcn$^+$ and ferricyanide shows mild pH dependence.

oxidation should be indicative on the intermediates and dominant pathways. A few $\mu$L from the ferricenium stock (10 mM) was injected into a 2 mL volume of the aqueous solution of $UQ_0H_2$ during heavy stirring (Figure 5). The rate of product formation was measured by an absorption change of the sample at 620, 280, and/or 249 nm, the characteristic peaks of the ferricenium/ferrocene difference spectrum (see Figure 2, bottom). The concentrations of the reactants were changed in a wide range (1−40 $\mu$M for ferricenium and 1−400 $\mu$M for $UQ_0H_2$) to get readily observable reaction rates. The pH of the solution was adjusted and kept constant by the series of pH buffers (10 mM acetate, 2−2 mM Mes and Mops) and did not change significantly after injection of the acidic solution of ferricenium. By keeping the pH in the acidic and neutral range, the rate of decomposition of ferricenium was much smaller than the rate of oxidation of the quinol. The bimolecular rate constant was determined from the observed initial rate and the concentrations of the reactants and plotted as a function of pH. The data align to a straight line of slope +1 (double logarithm plot of rate vs $[H^+]$) that has a tendency to level off at the highly acidic pH range. The autocatalytic oxidation of $UQ_0H_2$ does not play here an essential role, as addition of quinone ($UQ_0$) to the solution does not increase the rate of oxidation.

It is interesting to compare the bimolecular rate constants of $UQ_0H_2$ oxidation to fcn$^+$ and cyt $c^{3+}$. In both cases, the rate constants increase steeply with a slope of +1.0 at not too acidic pH values. The corresponding rate constants are 2−3 orders of magnitude higher for the fcn$^+$ than for the cyt $c^{3+}$.

**3.4. Electron Transfer from Quinol to Ferricenium Generated by Light-Excited RC.** The interacting redox species can be generated not only chemically but also photochemically by light excitation of the RC protein isolated from photosynthetic bacteria. As a consequence of the two-electron gate function of the bacterial RC, one molecule of $QH_2$ and two molecules of ferricenium are produced after two saturating flashes. Although the protein has marked absorption bands on the whole spectral range from UV to near IR, the kinetics of the redox equivalents established by light excitation can be separately measured and their kinetics can be compared even in the presence of the RC. The redox reaction between quinol and fcn$^+$ can be tracked by direct optical observation of the disappearance of the ferricenium (at 249 nm) or of the liberation of $H^+$ ions accompanying the quinol oxidation by pH indicator dyes (Figure 6a). Within the limit of the accuracy of our measurements, the initial rate constant of disappearance of ferricenium ($k'[fcn^+]$) is half of that of quinol ($k'[QH_2]$), indicating the common source (mutual redox reaction) of consumption of the reactants (data not shown). Notice the different initial slopes (decay rates) after the first and the second flashes in Figure 6a (trace without ferrocyanide). Although the (Bohr) proton taken up after the first flash is relatively stable, the two (chemical) protons in the quinol generated after the second flash, have much shorter lifetimes. Indeed, the kinetics of disappearance of these protons represents different chemical reactions: the oxidation of semiquinone and quinol, respectively. After even numbers of closely (1 s) spaced flashes larger than two, the quantity of the photoproduced reactants will be larger and consequently the observed initial rates of the decay will be proportionally larger (data not shown).

The rates were measured at different pH values, and the bimolecular rate constants between flash induced quinol ($UQ_0H_2$) and ferricenium in detergent (0.03% TX-100) solution were calculated (Figure 5.). Although the sensitivity of the pH indicator dyes used in this study cover a relatively narrow pH range ($6.5 < pH < 8.5$), the data of proton measurements in the presence of RC line up to the data set obtained for $UQ_0H_2$ oxidation by externally added fcn$^+$ without RC at lower pH values. The points at higher pH values show considerable scattering but follow the tendency along a straight line of slope +1. That is an obvious indication of the common nature of a chemical redox reaction between $UQ_0H_2$ and fcn$^+$ in aqueous solution with and without RC. It is arbitrary whether the species is produced by a protein (via light reaction) or added externally to the solution.

Three different electron donors to RC were applied to see how effective they are in their oxidized redox states to direct oxidation of $UQ_0H_2$ (Figure 5). Cytochrome $c^{2+}$ is the kinetically best suited (fastest) electron donor to $P^+$: its donation rate is at least 3 orders of magnitude larger than that of the ferrocene.[6,12] However, cytochrome $c^{3+}$ can oxidize $UQ_0H_2$ 3 orders of magnitude slower than ferricenium. Ferrocyanide is a very poor electron donor to the RC, and a very large concentration (≈100 mM) is needed to get a larger donation rate than that of the $P^+Q_B^- \rightarrow PQ_B$ charge recombination (≈ 1 $s^{-1}$). Ferricyanide, however, oxidizes $UQ_0H_2$ somewhat faster than ferricytochrome (but much slower than ferricenium).

The picture is significantly modified if $UQ_{10}$ is used instead of (water soluble) $UQ_0$ both in the $Q_B$ site of RC and in the quinone pool. In sharp contrast to the steep pH dependence of the rate of $UQ_0H_2$ oxidation by fcn$^+$ (slope of +1), the bimolecular rate constants between flash induced ubiquinol-10 ($UQ_{10}H_2$) and ferricenium did show only mild pH dependence (slope of 0.25/pH unit, Figure 5). Although in a much more restricted pH range, negligible pH dependence was observed using ferricyanide as an electron acceptor to $UQ_{10}H_2$. The observed difference in magnitude and pH dependence of the

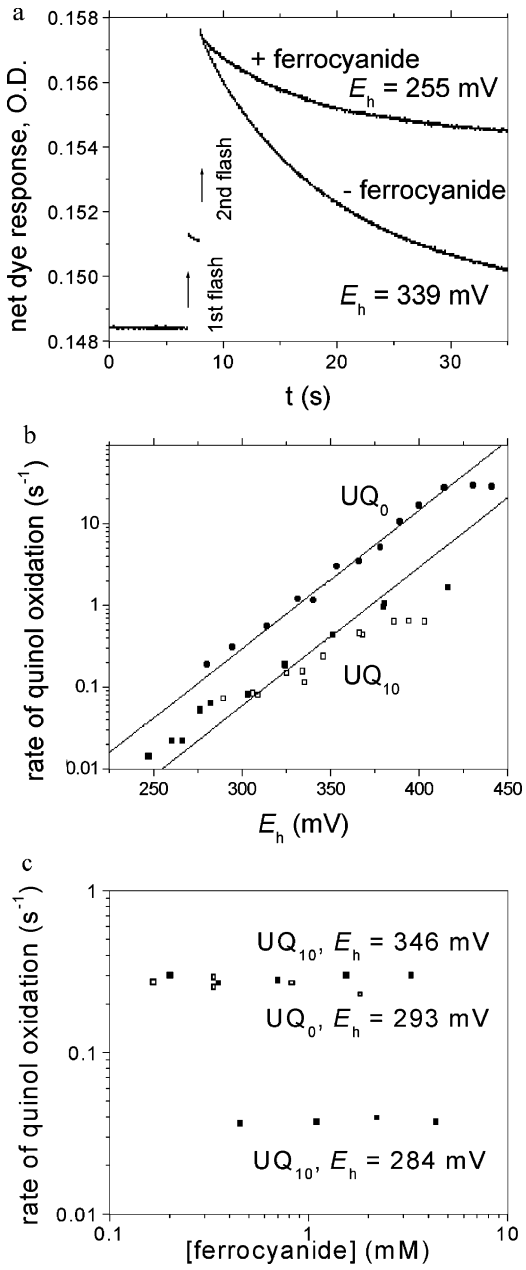


**Figure 6.** The role of ferrocyanide in oxidation of quinol ($UQ_0H_2$ and $UQ_{10}H_2$) by ferricenium generated in bacterial RC after two saturating flashes. The rate of oxidation was determined from the kinetics of acidification of the solution detected by response of pH indicator dye. (a) Kinetic traces of quinol oxidation. Conditions were as follows: 1.5 $\mu$M RC, 20 $\mu$M $UQ_{10}$, 20 $\mu$M phenol red, detection wavelength 562 nm, 30 mM KCl, 100 $\mu$M ferrocene, 0.03% TX-100, pH 7.0, and $E_h$ = 339 mV (no ferrocyanide) and 255 mV (with 5 mM ferrocyanide). (b) Actual redox potential ($E_h$) dependence of the rate of quinol ($UQ_0H_2$ and $UQ_{10}H_2$) oxidation by ferricenium. The actual redox potential was adjusted by ferri/ferrocyanide (■, ●) and $H_2O_2$ (□). The fit lines were derived from eq 18 using $E_m$ ($fcn^+$/fcn) = 400 mV and $k'$[fcn] = 15 $s^{-1}$ (for $UQ_0$) and $k'$[fcn] = 3.0 $s^{-1}$ (for $UQ_{10}$) (see details in the text). Conditions were as follows: 1.5 $\mu$M RC, 0.03% TX-100, 100 $\mu$M ferrocene, 25 mM NaCl, and 10 $\mu$M $UQ_{10}$ [pH 8.0 and 30 $\mu$M *o*-cresol red (observation wavelength 572 nm and ± 10 mM Tris)] or 500 $\mu$M $UQ_0$ [pH 6.5 and 30 $\mu$M BCP (observation wavelength 579 nm and ± 10 mM Mes)]. (c) Observed rate of quinol oxidation by ferricenium as a function of concentration of ferrocyanide added in constant ratio with ferricyanide to keep the actual redox potential of the solution constant ($E_h$ = 284, 293, and 346 mV). The quinone was either $UQ_0$ (□) or $UQ_{10}$ (■). Conditions were as follows: 1.5 $\mu$M RC, 0.03% TX-100, pH 8.0, 100 $\mu$M ferrocene, 25 mM NaCl, 30 $\mu$M *o*-cresol red (detection wavelength 572 nm and ±10 mM Tris) and 10 $\mu$M $UQ_{10}$ or 500 $\mu$M $UQ_0$.

rates of oxidation of $UQ_0H_2$ and $UQ_{10}H_2$ highlights the significance of their partition in a heterogeneous system and the difference in the oxidation pathways.

By screening the electrostatic interaction among charged reactants, modification of the ionic strength of the solution serves as a useful tool in our hands to study the mechanism of quinol oxidation. Similarly to the pH dependence of the rate of quinol oxidation, the ionic strength dependence showed marked difference if water soluble $UQ_0$ or hydrophobic $UQ_{10}$ occupied the $Q_B$ site of the RC (Figure 7, left). The ionic strength of the solution was increased up to 100 mM, and the rate of quinol oxidation was measured by two different methods. The quinol was produced photochemically after two saturating flashes, and its oxidation was tracked by disappearance of ferricenium (285 nm) or by acidification of the solution monitored by pH indicator dyes. If the $Q_B$ site was reconstituted by $UQ_0$, the rate of quinol oxidation followed the Debye−Hückel theory (a slope of −1 was obtained in representation of the logarithm of the rate vs square root of the ionic strength), and the slope was independent of the pH of the solution. In the case of the native quinone ($UQ_{10}$), however, a much smaller slope was obtained (pH 6.5) that showed strong pH dependence (Figure 7, right). Below pH 6, the slope turned from negative to positive. The observed difference is a strong indication of involvement of electrically different species in the reaction route of quinol oxidation. Additionally, focusing/defocusing electrostatic effect of the protein surface charge on the partners in the redox reaction may be involved as the observed pH range includes the isoelectric point of the RC.[30]

The concentration of the redox partners can be changed by adjustment of the actual redox potential ($E_h$), and consequently, the kinetic parameters will be also altered. Indeed, the observed rate of quinol oxidation (measured as the acidification of the solution) showed characteristic dependence on $E_h$ set by different redox mediators (Figure 6b). Although the $E_h$ was increased, the rate monotonously increased. At high oxidizing potentials ($E_h$ > 450 mV), the kinetic separation of (fast and efficient) electron donation to $P^+$ by ferrocene and (slow) quinol oxidation by ferricenium runs into difficulties; therefore, this potential is considered as the upper limit in our experiments. In semilogarithm representation and at room temperature, the linear phase had a slope of close to 1/59 $mV^{-1}$. The curves measured for two different types of quinones ($UQ_0$ and $UQ_{10}$) and at different pH values showed similar behavior except in the difference of the actual rates: for $UQ_0$, higher rates were obtained than for $UQ_{10}$ in accordance with the results in Figure 5.

Ferrocyanide decelerated the quinol oxidation (Figure 6a). Addition of 5 mM ferrocyanide slowed down significantly the acidification of the solution due to quinol oxidation. As the oxidation rate depends strongly on the actual redox potential (Figure 6b), ferrocyanide may act via efficient redox interaction (mediation): upon addition of ferrocyanide, the concentration of ferricenium decreases, which lowers the initial rate of quinol oxidation. This is demonstrated in Figure 6c, where the rate of quinol oxidation is measured as a function of ferrocyanide concentration under constant redox potential. (The stability of the redox potential could be achieved above 0.1 mM ferrocyanide.) Interestingly, the rate of quinol oxidation by ferricenium did not depend on the ferrocyanide concentration but only on the actual redox potential.

## 4. Discussion

**4.1. Stability of Ferricenium/Ferrocene in Aqueous Solutions.** It was clearly demonstrated that the ferrocene had limited

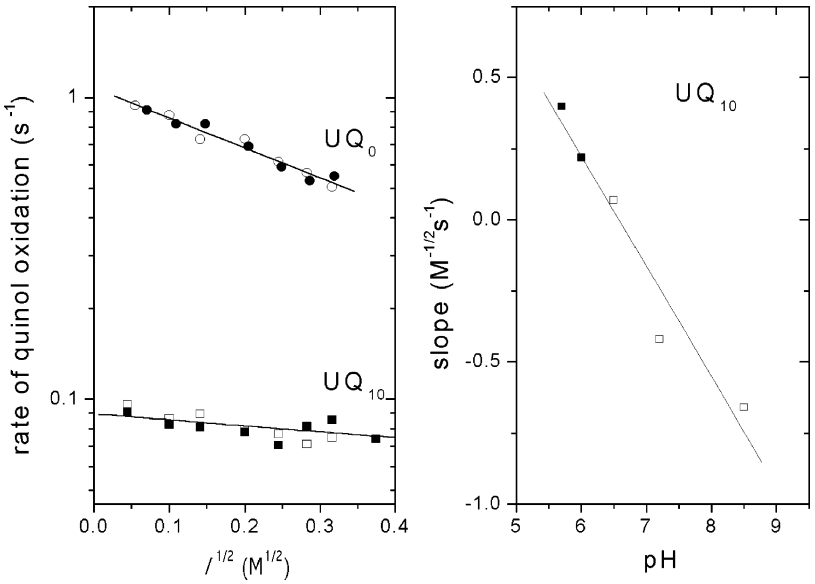


**Figure 7.** Ionic strength dependence of the rate of quinol ($UQ_0H_2$ and $UQ_{10}H_2$) oxidation by ferricenium (left panel) and the pH dependence of the slope of the ionic strength dependence of $UQ_{10}H_2$ oxidation (right panel). The quinol was generated by two saturating flashes in bacterial RC, and the rate of its oxidation was monitored by pH indicator dyes (open symbols) or by disappearance of the ferricenium (285 nm, closed symbols). The ionic strength of the solution was adjusted by KCl. The observed rate for $UQ_0$ was corrected for the rate of reaction via $UQ_0H_2$ (see the text and Figure 5). The slope of the best fit straight line for $UQ_0$ is $-1.0$ $M^{-1/2}$ $s^{-1}$ (left panel) and shows a monotonous drop by increasing pH for $UQ_{10}$ (right panel). Conditions were as follows: 1 $\mu$M RC, 0.02% TX-100, 100 $\mu$M ferrocene, 50 $\mu$M (●) or 500 $\mu$M (○) $UQ_0$, 10 $\mu$M $UQ_{10}$ (■, □), 20 $\mu$M pH indicator dye (○, □), 1 mM buffer (●, ■), and pH 7.0 (left panel).

solubility in aqueous solution and the ferricenium cation was stable in highly acidic aqueous solution but decomposed in neutral or basic solutions. The kinetics of disappearance of ferricenium was followed optically by simultaneous loss of unsolubilized ferrocene in the aqueous solution (Figure 3). Cyclic voltammograms (CV) of the ferricenium/ferrocene redox couple at different pH values indicated the increasing extent of irreversible change of the CV upon increase of the pH: at very low pH (or if the ferricenium was encapsulated in the protein pocket), reversible CV was measured with a cathodic-to-anodic peak current ratio ($i_{pc}/i_{pa}$) close to 1 that decreased to 0.41 at pH 4 and further decreased to 0.22 at pH 7.[14] The ferricenium ion (having 17 electrons rather than 18 electrons in its shell) turned out to be susceptible to nucleophilic attack by even very weak nucleophiles (like water); therefore, its lifetime depended on the quality and concentration of nucleophilic agents including the hydroxide ion ($OH^-$) at high pH or small anions as simple as $Cl^-$, $I^-$, or $Br^-$ in the solution[31] or phosphate. The observed instability is not very much surprising, as only few metal-containing redox couples are stable in both oxidized and reduced states in water. One well-known exception is the redox pair of ferri/ferrocyanide, which is frequently used in electrochemical studies of water soluble biomolecules.

The mechanism as how ferricenium decomposes is a very complex process involving many products. The different views about the decomposition reactions and the nature of the decomposition products have a common point of ligand exchange around the $Fe^{3+}$ ion.[31] (To refer to the structures, ferrocene and ferricenium are symbolized as $FeCp_2$ and $FeCp_2^+$ in eqs 1−4, respectively; the usual symbols fcn and $fcn^+$ will be used otherwise.)

$$FeCp_2^+ + nL \leftrightarrow FeL_n^{3+} + 2Cp^- \qquad (1)$$

Here, Cp is the cyclopentadienyl ring; L is a nucleophilic ligand that can be a solvent molecule, a neutral species, or a mononegative anion; and $n$ is an integer number. As the generated $Cp^-$ anions have high reducing power, the $Fe^{3+}$ complexes will be easily reduced in the solution:

$$Cp^- + FeCp_2^+ \leftrightarrow Cp^0 + FeCp_2 \qquad (2a)$$

$$Cp^- + FeL_n^{3+} \leftrightarrow Cp^0 + FeL_n^{2+} \qquad (2b)$$

(Here, the symbol $^0$ stays for the unpaired electron of Cp.) The cyclopentadienyl radicals $Cp^0$ will combine to $Cp_2$ or abstract hydrogen atoms from solvent molecules to form cyclopentadiene, which will dimerize to $C_{10}H_{12}$:

$$2C_5H_5 \rightarrow C_{10}H_{10} \text{ or } C_{10}H_{12} \qquad (3)$$

On the other side, $Cp^-$ can immediately react in aqueous solution with $H_2O$, $OH^-$, or $H^+$ by delivering several side products.[32]

$$\left.\begin{array}{l} Cp^- + H_2O \\ Cp^- + OH^- \\ Cp^- + H^+ \end{array}\right\} \rightarrow \text{side products} \qquad (4)$$

According to reaction (1), the strength of the donor will determine the position of the ligand exchange equilibrium, i.e., whether the $fcn^+$ cation will decompose or not. The competition between L and $Cp^-$ ligands for the $Fe^{3+}$ ion is not fair, and consequently, no simple predictions can be made on the basis of the donor strengths. The observed stability of $FeCp_2^+$ in acidic solution and its decomposition in alkaline solution indicate that the donor strength of water ($L = H_2O$) is insufficient, whereas the donor strength of the $OH^-$ ions ($L = OH^-$) proves to be sufficient for decomposition of the ferricenium.

The major reactions of the ferricenium/ferrocene redox couple in aqueous solution can be summarized as

$$\mathrm{fcn}_{(us)} \underset{\text{fast}}{\overset{\text{solubility}}{\rightleftharpoons}} \mathrm{fcn}_{(sol)} \underset{\text{fast}}{\overset{E_h}{\rightleftharpoons}} \mathrm{fcn}^+_{(sol)} \xrightarrow[\text{slow}]{\text{pH, nucleophile}} \text{ligated form}_{(sol)} \quad (5)$$

The solid suspension of unsolubilized ferrocene ($fcn_{(us)}$) is in fast equilibrium with its dissolved form ($fcn_{(sol)}$). The equilibrium constant is determined by the solubility of the ferrocene in water (Figure 3).[23,29] The ferrocene in solution is in fast redox equilibrium with its oxidized form that will undergo nucleophilic attack in which $OH^-$ or any nucleophile will ligate to the iron expelling the cyclopentadienyl rings. The rate of this reaction depends on pH and the type and concentration of the nucleophile in the solution. Different methods can be used to protect the ferricenium from the solvent, thus to eliminate the reaction of ligation. It can be encapsulated inside proteins by covalent attachment to the active site of azurin,[14] caged in a cyclic oligosaccharide, incorporated in micelles of non-ionic detergents,[28] or stabilized by a counterion ($fcn^+PF6^-$). In the majority of our kinetic experiments, we did not protect the ferricenium from the solvent by any of the sophisticated methods because its rate of decomposition could be kept smaller than that of the electron transfer from quinol at all pH values used in our study.

**4.2. Pathways of Quinol Oxidation by Ferricenium and Difference between Oxidation of $UQ_0H_2$ and $UQ_{10}H_2$.** In aqueous solution, the fully reduced and protonated quinone ($QH_2$) goes to the fully oxidized form (Q) in a concerted two electron and two proton reaction.[16] There are nine possible intermediates that can be arranged according to their redox and protonation states (Figure 8). The different protonated forms of the quinol play an essential role in the autocatalytic and non-autocatalytic reduction of ferricenium. The dihydroquinone ($QH_2$) may lose both protons in consecutive reactions of equilibrium constants of $K_A$ and $K_B$, respectively:

$$QH_2 \overset{K_A}{\longleftrightarrow} QH^- + H^+ \quad (6)$$

$$QH^- \overset{K_B}{\longleftrightarrow} Q^{2-} + H^+ \quad (7)$$

Under steady-state conditions, the concentrations of the monoprotonated and the completely deprotonated forms of the quinol can be calculated

$$[QH^-] = \frac{[QH_2]_{tot}}{1 + 10^{pH-pK_B} + 10^{pK_A-pH}} \quad (8)$$

$$[Q^{2-}] = \frac{[QH_2]_{tot}}{1 + 10^{pK_B-pH} + 10^{pK_B+pK_A-2pH}} \quad (9)$$

where $[QH_2]_{tot}$ is the total quinol concentration in the system. In the pH range of pH $\ll$ p$K_A$, p$K_B$, the logarithms of $[QH^-]$ and $[Q^{2-}]$ are steep functions of pH with slopes of +1 and +2, respectively.

The quinol can be oxidized by the quinone itself in several steps. The double anionic form ($Q^{2-}$) is readily oxidized by quinone (dismutation, bimolecular rate constant $k'_d$) to anionic semiquinone ($Q^-$), which is further oxidized by transfer of its electron to a not well identified electron acceptor (e.g., oxygen) in the aqueous solution[9] (rate constant $k_s$, not shown in Figure 8):

$$Q^{2-} + Q \xrightarrow{k'_d} 2Q^{\bullet -} \xrightarrow{k_s} 2Q + 2e^- \quad (10)$$

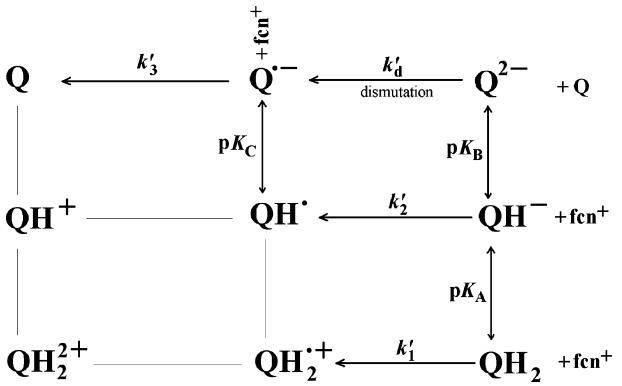


**Figure 8.** Redox and protonation states of quinones (Q). The possible ways of electron transfer (horizontal arrows with bimolecular rate constants $k'$) and proton transfer (vertical arrows with proton equilibrium constants $K$) among quinone intermediates are indicated upon oxidation of quinol by quinone (dismutation) or ferricenium ($fcn^+$).

In our experiments (Q = $UQ_0$), the initial rate of quinone accumulation was determined from the initial slope of the kinetics: $k_d = 0.39\ \mu M\ UQ_0/min$ (Figure 4). This result can be used to derive the bimolecular rate constant of the $UQ_0H_2 \rightarrow UQ_0$ redox reaction ($k'_d$). If the observed rate is limited by the rate of dismutation, then

$$k_d = k'_d[UQ_0^{2-}][UQ_0] \quad (11)$$

Insert eq 9 into eq 11:

$$k_d = \frac{k'_d[UQ_0H_2]_{tot}[UQ_0]}{1 + 10^{pK_B-pH} + 10^{pK_A+pK_B-2pH}} \quad (12)$$

We used equimolar (initial) concentrations of $[UQ_0]$ (= 50 $\mu$M) and $[UQ_0H_2]_{tot}$ (= 50 $\mu$M), and the p$K$ values of ubiquinol-0 were determined from Hammett's equation for the p$K$ of substituted phenols: p$K$ = 9.92−2.23$\Sigma\sigma_i$, where $\sigma_i$ is the Hammett constant for substituent $i$.[33] We calculated p$K_A$ = 10.03 and p$K_B$ = 12.43 that are close to p$K$ values of p$K_A$ (= 10.7) and p$K_B$ (= 12.7) established for $UQ_{10}$.[34] Because both p$K$ values are much larger than the actual pH value (= 6.9), the concentration of $UQ_0^{2-}$ (one reactant in the dismutation) is very small. This makes the observed rate very small, although the bimolecular rate constant of the dismutation is very large: $k'_d = 1 \times 10^{10}\ M^{-1}\ s^{-1}$ (Figure 4). The obtained value for $UQ_0$ is somewhat larger than that found for benzoquinone under slightly different conditions ($6.3 \times 10^8\ M^{-1}\ s^{-1}$).[15]

The electron transfer from quinol to ferricenium in solution involves bimolecular collision reactions between the partners (Figure 8). Three different mechanisms of reduction of ferricenium can be distinguished: collision reactions with quinol (bimolecular rate constant $k'_1$), anionic (deprotonated) quinol ($k'_2$), and anionic semiquinone ($k'_3$). The corresponding rates are

$$k_1 = k'_1[UQ_0H_2][fcn^+] \quad (13)$$

$$k_2 = k'_2[UQ_0H^-][fcn^+] \quad (14)$$

$$k_3 = k'_3[UQ_0^-][fcn^+] \quad (15)$$

The observed rate is the sum of the rates of these elementary processes. However, the actual rate is somewhat more complicated because the two-electron chemistry of the quinone should be coupled to the one-electron chemistry of the ferricenium/

ferrocene redox pair in the RC: the quinol will be oxidized by two subsequent collision reactions either with two ferricenium cations or with one ferricenium and one quinone (dismutation) molecules. The concentrations of the different redox and protonation states of the quinone can be determined from the protonation equilibrium (see eqs 8 and 9) and the pathway of reduction. For example, the semiquinone can be formed either by dismutation or by oxidation of the anionic quinol by ferricenium. The pH of the solution will determine the protonation states of the quinone; therefore, the method based on its change can be applied to identify the dominant pathways and rate constants of reduction of ferricenium by $QH_2$ in aqueous solution.

The actual bimolecular rate constants of the different routes can be deduced from comparison of the pH dependence of the observed rate constants (Figure 5) with the predictions of the quinol oxidation scheme (Figure 8 and eqs 8 and 9). In the case of $UQ_0$, we can argue that, in the very low pH range, the reduction of ferricenium is mediated by $UQ_0H_2$ as no pH dependence is observed. However, at higher pH values, the straight line with strict +1 slope indicates the contribution of the anionic (single deprotonated) quinol, $UQ_0H^-$. The involvement of the semiquinone anion ($UQ_0^-$) mediated route is negligible because the autocatalyzed reaction rate should show a pH dependence of slope +2 and should be stimulated by the presence of small amounts of quinone in the reaction mixture. Neither of these two predictions was observed in our experiments. The bimolecular rate constant can be expressed by the pH dependence of $[QH^-]$:

$$k' = k'_1 + \frac{k'_2}{1 + 10^{\mathrm{pH}-\mathrm{p}K_B} + 10^{\mathrm{p}K_A-\mathrm{pH}}} \qquad (16)$$

and thus the $k'_1$ and $k'_2$ bimolecular rate constants can be determined by a fitting procedure. The p$K$ values of ubiquinol-0 ($pK_A = 10.03$ and $pK_B = 12.43$) were calculated from Hammett's equation (see above). The fit offered $k'_1 = 65\ M^{-1}\ s^{-1}$ and $k'_2 = 5 \times 10^8\ M^{-1}\ s^{-1}$ for ferricenium and $k'_1 \ll 10\ M^{-1}\ s^{-1}$ and $k'_2 = 1.5 \times 10^5\ M^{-1}\ s^{-1}$ for ferricytochrome. Probably due its smaller molecular size (and higher redox midpoint potential), the ferricenium (/ferrocene, $E_m = 400$ mV at pH 7) oxidizes the quinol much faster than cyt $c^{3+}$ (/cyt $c^{2+}$, $E_m = 220$ mV at pH 7) on both pathways mediated by $UQ_0H_2$ and $UQ_0H^-$.

The ionic strength dependence of the observed rate gave further support for involvement of the anionic form of the quinol in its oxidation by $fcn^+$ (Figure 7). As $UQ_0H_2$ and $UQ_0H^-$ differ in charge, the increase of ionic strength ($I$) should cause marked decrease in rate of reaction mediated by $UQ_0H^-$ according to the Debye−Hückel expression for dilute ionic solution:

$$\log k_{QH^-} = \log k(I = 0) + 1.02 z_{QH^-} z_{fcn^+} \sqrt{I} \qquad (17)$$

and has no effect on the rate if the route is via $UQ_0H_2$ (neutral quinol). As $z_{QH^-} = -1$ and $z_{fcn^+} = +1$, a slope of −1.02 should be obtained. Indeed, we got a slope of −1.0 at any pH if the water soluble $UQ_0$ was used.

The experiments with $UQ_{10}$, however, did show a different pattern. Both the pH and the ionic strength dependences deviated from those obtained for $UQ_0$. Neither the pH (Figure 5) nor the ionic strength (Figure 7) had much influence on the rate, and mild slopes were obtained. As a possible explanation, the dramatic changes of the p$K_A$ and p$K_B$ values can be excluded as similar values were reported for $UQ_0$ and $UQ_{10}$ (see above). The observed difference in the rates and pH dependence of oxidation of $UQ_0H_2$ and $UQ_{10}H_2$ by $fcn^+$ may come from two sources.

(1) It can originate from the heterogeneity of the (detergent) system together with the hydrophilic and hydrophobic nature of $UQ_0$ and $UQ_{10}$, respectively. Anchored to the micelles by its hydrophobic chain, the different redox states of $UQ_{10}$ are not readily available to the aqueous (bulk) phase; therefore, smaller rates than those of water soluble $UQ_0$ are expected with $fcn^+$ (Figure 5).

(2) The bimolecular rate constants ($k'$) of the oxidation routes (Figure 8) could be different for the two quinone species favoring the path through the neutral quinol ($UQ_{10}H_2$) and disfavoring the reaction via the anionic quinol ($UQ_{10}H^-$). However, the rate showed slight pH dependence, and the slope of the ionic strength dependence determined from eq 17 demonstrated also pH dependence: it was very small at pH 6.5 and became larger at increase (more negative) or decrease (more positive) of the pH (Figure 7 right). Because the marked change occurred around the isoelectric point of the RC measured[30] and calculated[35] as p$I$ = 6.1, we attribute the observation to the influence of the surface electrostatics of the RC protein on the charged reactant (ferricenium). At a pH close to the p$I$ of the protein, the RC is neutral and has no electrostatic influence on the rate of quinol oxidation. However, if pH > p$I$, the protein is net negatively charged and accelerates the ferricenium to the micelle where $UQ_{10}H_2$ is located. In this way, the RC facilitates the increase of the rate of the quinol oxidation. Addition of salt will screen the surface charge of the RC and diminish the rate of quinol oxidation. The higher the pH, the larger will be the negative surface potential of the RC. A similar effect but with opposite sign occurs when pH < p$I$. A related effect of acceleration of $H^+$ uptake kinetics in wild-type RCs was shown earlier.[36] Salts caused a substantial slowing of $H^+$ uptake by the $P^+Q_A^-$ state, i.e., in the absence of any rate-limiting electron transfer. High salt concentrations were required for this effect at alkaline pH, and this was taken to indicate a substantial surface charge density, qualitatively consistent with the large number of ionizable residues in the RC cytoplasmic domain.

**4.3. Deceleration of Quinol Oxidation by Ferrocyanide.** It was demonstrated that ferrocyanide effectively stabilized the photochemically produced quinol (Figure 6a). The rate of quinol oxidation by ferricenium decreased by factors of 3−4 in the presence of excess amount of ferrocyanide. On the other hand, it was shown that the interaction of ferricyanide with quinol is extremely weak (Figure 5). We argue that the ferrocyanide does not have a unique property to protect the quinol from oxidation, but it acts via modification (decrease) of the actual redox potential. This is the way it controls the concentration of the ferricenium so that it is an efficient oxidant for the quinol. Because the oxidation of quinol by ferricenium occurs via collision reaction, the initial (monoexponential) rate constant of the ferricenium−quinol bimolecular reaction is at room temperature

$$k^{ox}_{QH_2} = k'[fcn^+] = k'[fcn]10^{(E_h - E_m)/59\mathrm{mV}} \qquad (18)$$

where $k'$ is the bimolecular rate constant and $[fcn^+]$ is expressed by the Nernst equation. As ferrocene is added in large excess to the solution, [fcn] is the solubility limit of ferrocene in water (42 $\mu$M). The logarithm of the observed rate constant is the linear function of the actual redox potential with a slope of $(59\ \mathrm{mV})^{-1}$:

$$\log k_{QH_2}^{ox} = \frac{E_h}{59\ mV} + \text{const} \qquad (19)$$

Indeed, this dependence was obtained under different conditions (type of quinones and pH). The measured points in Figure 6b were fitted by eq 18 with an adjustable parameter of $k'$ in the case of both quinones ($E_m = 400$ mV). Acceptable coincidence between data and calculated values were obtained by $k' = 7.1 \times 10^4\ M^{-1}\ s^{-1}$ (for $UQ_{10}$) and $k' = 3.6 \times 10^5\ M^{-1}\ s^{-1}$ (for $UQ_0$). The bimolecular rate constants are close to those found from pH dependence of the quinol oxidation rate (Figure 5).

Upon light excitation of the RC, the redox agents (quinol and ferricenium) are produced in pairs and emerge pair-wise from the same protein. However, the establishment of the redox equilibrium is so fast and the electron transfer from quinol to photoproduced ferricenium is so slow that they do not interact directly. They spread out the bulk before the actual quinol → ferricenium electron transfer can take place. As consequence of the relatively long lifetime ($t_{1/2} > 1$ s) of the species, they will distribute by diffusion randomly in the solution. The mean displacement by diffusion in three dimensions amounts to $\sqrt{6Dt_{1/2}} = 25\ \mu$m (the diffusion coefficient is taken $D = 100\ \mu m^2\ s^{-1}$), which is about 2 orders of magnitude larger than the mean distance (0.1 $\mu$m) among neighboring RC molecules ([RC] = 1 $\mu$M). Thus, the approach of bimolecular collision of randomly distributed species is an adequate description of the mechanism of the electron transfer between the quinol and the ferricenium.

**Acknowledgment.** We are grateful for the financial support of OTKA (TO42680), Balaton (F-4/04), and the MTA-CNR bilateral agreement. LG was supported by the Bolyai fellowship. Many thanks to Nicola De Nicolò (Universitá di Bari) for his help in the construction of Figure 5, to Pinalysa Cosma (Universitá di Bari) for the cyclic voltammetry measurement on ferrocene, and to Yan-Yeung Luk (Departments of Chemistry and Biomedical and Chemical Engineering, Syracuse University, New York) for his interest in this study.

## References and Notes

(1) Paddock, M. L.; Feher, G.; Okamura, M. Y. *FEBS Lett.* **2003**, *555*, 45.
(2) Wraight, C. A. *Front. Biosci.* **2004**, *9*, 309.
(3) Wraight, C. A. *Biochim. Biophys. Acta* **2006**, *1757*, 886.
(4) McPherson, P. H.; Okamura, M. Y.; Feher, G. *Biochim. Biophys. Acta* **1990**, *1016*, 289.
(5) Osváth, Sz.; Maróti, P. *Biophys. J.* **1997**, *73*, 972.
(6) Gerencsér, L.; Laczkó, G., Maróti, P. *Biochemistry* **1999**, *38*, 16866.
(7) Van Rotterdam, B. J.; Westerhoff, H. V.; Visschers, R. W.; Bloch, D. A.; Hellingwerf, K. J.; Jones, M. R.; Crielaard, W. *Eur. J. Biochem.* **2001**, *268*, 958.
(8) Gerencsér, L.; Maróti, P. *Biopolymers* **2004**, *74*, 96.
(9) Gerencsér, L.; Maróti, P. *Biochemistry* **2006**, *45*, 5650.
(10) Van Rotterdam, B. J. *Ph.D. Thesis.* Universiteit van Amsterdam: Amsterdam, 1998.
(11) Van Rotterdam, B. J.; Westerhoff, H. V.; Visschers, R. W.; Jones, M. R.; Hellingwerf, K. J.; Crielaard, W. *Biophys. Chem.* **2000**, *88*, 137.
(12) Maróti, P.; Wraight, C. A. *Biochim. Biophys. Acta* **1988**, *934*, 329.
(13) Nielson, R. M.; Golovin, M. N.; McManis, G. E.; Weaver, M. J. *J. Am. Chem. Soc.* **1988**, *110*, 1745.
(14) Hwang, H. J.; Carey, J. R.; Brower, E. T.; Gegenbach, A.; Abramite, J. A.; Lu, Y. *J. Am. Chem. Soc.* **2005**, *127*, 15356.
(15) Rich, P.; Bendall, D. S. *Biochim. Biophys. Acta* **1980**, *592*, 506.
(16) Rich, P.; Bendall, D. S. *FEBS Lett.* **1979**, *105*, 189.
(17) McPherson, P. H.; Okamura, M. Y.; Feher, G. *Biochim. Biophys. Acta* **1993**, *1144*, 309.
(18) Agostiano, A.; Mavelli, F.; Milano, F.; Giotta, L.; Trotta, M.; Nagy, L.; Maróti, P. *Bioelectrochemistry* **2004**, *63*, 125.
(19) Milano, F.; Gerencsér, L.; Agostiano, A.; Giotta, L.; Nagy, L.; Trotta, M.; Maróti, P. *Photosynthesis: Fundamental Aspects to Global Perspectives*; van der Est, A., Bruce, D., Eds.; International Society of Photosynthesis, 2005; p 213.
(20) Dorogi, M.; Bálint, Z.; Mikó, Cs.; Vileno, B.; Milas, M.; Hernádi, K.; Forró, L.; Váró, Gy.; Nagy, L. *J. Phys. Chem. B.* **2006**, *110* (43), 21473.
(21) Morrison, L. E.; Schelhorn, J. E.; Cotton, Th. M.; Bering, C. L.; Loach, P. A. *Function of Quinones in Energy Conserving Systems*; Academic Press, Inc.: New York, 1982; p 35.
(22) *CRC Handbook of Chemistry and Physics*, 74th ed.; Lide, D. R., Ed.; CRC Press: Boca Raton, FL, 1993−1994; pp 8−23.
(23) Georges, J.; Desmettre, S. *Electrochim. Acta **1984**, 29*, 521.
(24) Rosen, D.; Okamura, M. Y.; Feher, G. *Biochemistry* **1980**, *19*, 5687.
(25) Okamura, M. Y.; Isaacson, R. A.; Feher, G. *Proc. Natl. Acad. Sci. U.S.A.* **1975**, *72*, 3491.
(26) Agostiano, A.; Milano, F.; Trotta, M. *Eur. J. Biochem.* **1999**, *262*, 358.
(27) Togni, A.; Hayashi, T. *Ferrocenes: Homogeneous catalysis, Organic Synthesis, Materials Science*; Wiley-VCH: Weinheim, Germany, 1975.
(28) Fujihira, Y.; Kuwana, Th.; Hartzell, C. R. *Biochem. Biophys. Res. Commun.* **1974**, *61* (2), 538.
(29) Abraham, M. H.; Benjelloun-Dakhama, N.; Gola, J. M. R.; Acree, W. E.; Cain, W. S.; Cometto-Muniz, J. E. *New J. Chem.* **2000**, *24*, 825.
(30) Prince, R. C.; Cogdell, R. J.; Crofts, A. R. *Biochim. Biophys. Acta* **1974**, *347*, 1.
(31) Prins, R.; Korswagen, A. R.; Kortbeek, A. G. T. G. *J. Organomet. Chem.* **1972**, *39*, 335.
(32) Holecek, J.; Handlir, K.; Pavlik, I. *Collect. Czech. Chem. Commun.* **1972**, *37*, 1805.
(33) Gordillo, G. J.; Schiffrin, D. J. *J. Chem. Soc., Faraday Trans.* **1994**, *90* (13), 1913.
(34) Zhu, Z.; Gunner, M. R. *Biochemistry* **2005**, *44*, 82.
(35) Takahashi, E.; Wraight, C. A. *J. Biol. Chem.* **2006**, *281* (7), 4413.
(36) Maróti, P.; Wraight, C. A. *Biophys. J.* **1997**, *73*, 367.